Correlation between physical properties and hydrogen concentration in magnetron-sputtered amorphous silicon

F. Demichelis, E. Minetti-Mezzetti, A. Tagliaferro, and E. Tresso
Dipartimento di Fisica del Politecnico di Torino, I-10129 Torino, Italy

P. Rava
Elettrorava Società per Azioni, I-10040 Savonera, Torino, Italy

G. A. Della Mea and P. Mazzoldi
Dipartimento di Fisica dell'Università degli Studi di Padova, I-35100 Padova, Italy
(Received 12 September 1985)

A study of the physical properties of α-Si:H films deposited by magnetron sputtering at two different substrate temperatures and different hydrogen content is presented. Quantitative depth profiles for hydrogen contents were determined by the use of the resonant nuclear reaction $^1H(^{15}N,\alpha\gamma)^{12}C$. The hydrogen concentration obtained by nuclear reaction is compared with the integrated intensities of the bond wagging, stretching, and bending bands. Information on the composition of the films (homogeneity of Si, concentrations of Ar and other impurities) was obtained by Rutherford backscattering analysis. The index of refraction, the extinction coefficient, and the band gap are extracted. Dark conductivities were also measured and are reported together with the obtained values of the activation energy. Information about the single oscillator energy, the dispersion energy, and the characteristic volume band energy is given.

I. INTRODUCTION

Hydrogenated amorphous silicon is currently undergoing intensive study focused on the role that the hydrogen content plays in its photoelectric properties. Several investigations on the optical, electrical, and structural properties of α-Si:H films have been published.[1-8] A review of the more recent literature is reported in Ref. 9. However, a systematic study of the optical and electrical properties of α-Si:H films prepared by magnetron sputtering, combined with the analysis of chemical bonding structure and composition obtained by resonant nuclear reactions and ir spectroscopy seems useful in order to give correlations among the different physical properties.

In this work the properties of two sets of rf magnetron sputtered α-Si:H films, selected among the many films produced, prepared using various hydrogen contents and different substrate temperature are described. The following measurements were made: (1) optical transmittance and reflectance in the uv—visible—near ir spectra, (2) film thickness, (3) electrical resistivity, (4) optical absorption in the ir region, and (5) absolute calibration of H content by means of nuclear reaction. The hydrogen concentrations obtained by nuclear reactions are compared with the integrated intensities of the ir wagging, stretching, and bending bands.

Correlations between the integrated absorption and the absolute hydrogen content are given. Optical absorption, optical band gap, index of refraction, resistivity, and activation energy, are correlated with hydrogen content.

Spectroscopic and band-structure models such as those of Wemple-DiDomenico[10] and Bahl and Bhagat[11] are used to analyze the optical parameters such as the dispersion energy, the average excitation energy (interband transition energies), and characteristic valence-band energy.

II. EXPERIMENTAL PROCEDURE

A. Deposition conditions

A variety of hydrogenated amorphous silicon films were deposited by rf magnetron sputtering from monocrystalline electronic grade silicon targets (of 12 cm diameter) of about 10 Ω cm resistivity in a high-purity argon-hydrogen mixture whose partial pressures were measured with a mass spectrometer. The magnetron sputtering increases the deposition rate significantly with respect to the diode sputtering. The hydrogen concentration in the gas mixture was varied from 0 to 20 vol%. The gas partial pressures are reported in Table I.

The targets were supplied with constant power densities of 3—4 W/cm^2. Deposition rates were typically in the range 1—2.5 Å/s. Distance between the targets and the substrates was maintained at 41 mm.

Four types of substrates were used to generate the data reported here: fused silica for uv—visible—near-ir spectrophotometric measurements, Corning 7059 glass for electrical and nuclear reactions (NR) measurements, graphite for Rutherford backscattering measurements, and finally floating-zone (FZ) crystalline silicon for ir measurements. Crystalline silicon, in addition to being transparent to ir radiation, has an index of refraction close to that of α-Si, so that the amplitude of interference fringes produced by the film diminishes, facilitating the analysis of the vibrational absorption bands.

TABLE I. Deposition conditions.

Sample	H_2 in the gas bottle (vol %)	P_t (10^{-3} mbar)	P_{pH_2} (mbar)	P_{bar} (10^{-3} mbar)	H_2 in the sputtering chamber (vol %)	Vacuum (10^{-6} mbar)	Target voltage (V)
Si-E30	0	4.15	0	4.15	0	6	520
Si-E31	3	4.38	3.51×10^{-4}	4.03	8	6	530
Si-E32	12	4.67	7.94×10^{-4}	3.87	17	6	530
Si-E33	20	4.95	1.24×10^{-3}	3.71	25	10	510
Si-E34	0	4.15	0	4.15	0	6	500
Si-E35	3	4.38	3.51×10^{-4}	4.03	8	6	500
Si-E36	12	4.67	7.94×10^{-4}	3.87	17	6	550
Si-E37	20	4.95	1.24×10^{-3}	3.71	25	5	535
Si-E45	0	7.89	0	7.89	0	10	700
Si-E46	3	8.33	6.66×10^{-4}	7.66	8	10	720
Si-E47	12	8.87	1.51×10^{-3}	7.36	17	7	760
Si-E48	20	9.4	2.36×10^{-3}	7.07	25	7	810
Si-E49	0	7.89	0	7.89	0	7	710
Si-E50	3	8.33	6.66×10^{-4}	7.66	8	9	760
Si-E51	12	8.87	1.51×10^{-3}	7.36	17	6	750
Si-E52	20	9.4	2.36×10^{-3}	7.07	25	6	730

B. Characterization of films

Optical transmittance and reflectance measurements were made in the uv—near-ir region with a Beckman model UV 5254 spectrophotometer. Transmittance measurements were made at normal incidence in the double-beam model. Reflectance measurements were performed with an angle of incidence of 20° and compared with the reflectance of standard mirrors calibrated in near normal incidence at the National Bureau of Standards, U.S. Department of Commerce (Washington, D.C.). Transmission ir spectra were recorded in the range 4000 to 400 cm^{-1} using a Perkin-Elmer 580-B spectrophotometer.

The film thickness was measured by Dektak II stylus displacements and by means of a Varian Interferometer for viewing Fizeau fringes. The impurities (Ar) concentration profiles in the film and the film thickness were investigated by Rutherford backscattering spectrometry (RBS) of 1.8 MeV He^{4+} ions scattered at 160°. Knowledge of the RBS cross section allows a "first-principles" determination of atomic concentration to be derived from the scattering spectra. Furthermore, RBS is a nondestructive technique and the heating or damage of the sample can be neglected owing to low current (<10 nA) used in the experiments. The $^1H(^{15}N,\alpha\gamma)\,^{12}C$ nuclear reaction,[12] having a strong narrow isolated resonance at 6.38 MeV (full width at half maximum ~1.8 keV) in its excitation function provides direct analysis of the H depth profiles. Measurement of the reaction yields as a function of the incident ^{15}N beam energy makes it possible to obtain H concentration at different depths inside these samples.

The depth resolution of the method is determinated by the width of the resonance, by the energy distribution of the incident beam and by the energy straggling of the incoming particles in the sample. The depth resolution was 20 Å at the surface and 100 Å at a depth of 0.1 μm. Finally the dark resistances were measured by a two probe method, using a nanovoltmeter and a picoamperometer (Keithley models 181 and 614, respectively). The electrodes have been made by aluminum deposition of the edges of the films. All the samples (for conductivity measurements) have been deposited on nonconductive glass.

III. RESULTS

Experimental results were obtained on sets of silicon films deposited with different hydrogen concentration and different argon pressure at substrate temperatures of 250 and 280 °C, respectively: a wide range of optical and electrical properties was found for these films.

A. Amount of hydrogen from NR measurements

Figure 1 shows the hydrogen profiles versus depth into the films for four samples deposited at different hydrogen

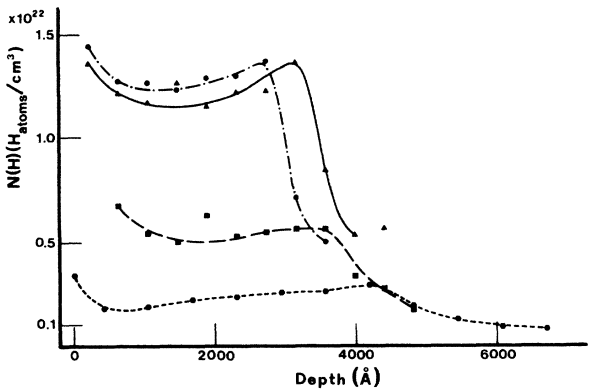

FIG. 1. Hydrogen depth profiles for samples Si-E45 (short-dashed line), Si-E46 (long-dashed line), Si-E47 (solid line), and Si-E48 (dashed-dotted line) deposited on Corning 7059 glasses.

TABLE II. Films characteristics and vibrational parameters.

Sample	Thickness (μm)	C(H) (at. %)	S_W (cm^{-1})	S_B (cm^{-1})	S_S (cm^{-1})	N(H) (at./cm^3)	$\frac{N(H)}{10^{19}S_W}$	$\frac{N(H)}{10^{20}S_B}$	$\frac{N(H)}{10^{20}S_S}$	$\frac{S_B}{S_S}$	$\frac{S_S}{S_W}$	$\frac{S_B}{S_W}$
Si-*E*34	2.3	~1	12.19			7.0×10^{20}	5.74					
Si-*E*35	2.3	9	313.87	6.03	37.41	4.5×10^{21}	1.43	7.46	1.20	0.16	0.12	0.02
Si-*E*36	2.0	23	384.11	10.63	56.49	1.15×10^{22}	2.99	10.8	2.04	0.19	0.15	0.03
Si-*E*37	2.0	29	411.09	11.45	70.41	1.45×10^{22}	3.53	12.1	2.06	0.16	0.17	0.03
Si-*E*49	3.2	4	28.17			2.0×10^{21}	7.10					
Si-*E*50	2.7	11	179.58		25.74	5.5×10^{21}	3.06		2.14	0.02	0.14	0.003
Si-*E*51	2.6	24	340.00	4.92	53.82	1.2×10^{22}	3.53	24.4	2.23	0.09	0.16	0.014
Si-*E*52	1.5	26	345.00	9.60	73.89	1.3×10^{22}	3.73	13.5	1.76	0.13	0.21	0.030

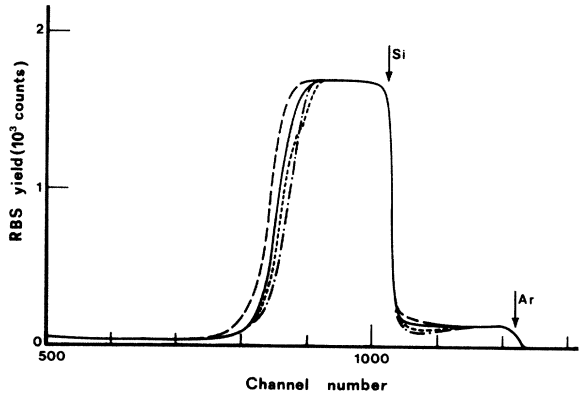

FIG. 2. RBS yield for samples Si-*E*45 (short-dashed line), Si-*E*46 (long-dashed line), Si-*E*47 (solid line), and Si-*E*48 (dashed-dotted line) deposited on graphite.

pressures p_H on Corning 7059 glasses at a temperature of the substrate of 250°C. A very good uniformity of the hydrogen distribution in the films can be observed. The film thicknesses shown in Fig. 1 are in excellent agreement with those obtained on graphite by means of the RBS, as they have been deduced from the Fig. 2. From this figure a value of 3—4 at. % for the argon content can also be deduced. The absolute values of the hydrogen concentration *C*(H) are reported in Table II.

B. ir Spectra

Absorption coefficients were calculated, starting from the recorded transmission spectra, taking into account the influence of the absorption due to the silicon substrate and of the interference fringes. The ir spectrum displays a bond-wagging (or rocking) band near 640 cm^{-1}, a bond-stretching band in the range 2000—2100 cm^{-1}, and a bond-bending band near 890 cm^{-1}. Also, a peak around 700 cm^{-1} can be observed in the samples with high hydrogen concentration (see Fig. 3). Brodsky *et al.*[2] identify this line in trisilane and the tetrasilanes with wagging of hydrogen in the triple complex SiH_3-SiH_2-SiH_3.

Figure 4 shows the absorption coefficients versus frequency for wagging and bending modes in films having different hydrogen concentration. The absorption coeffi-

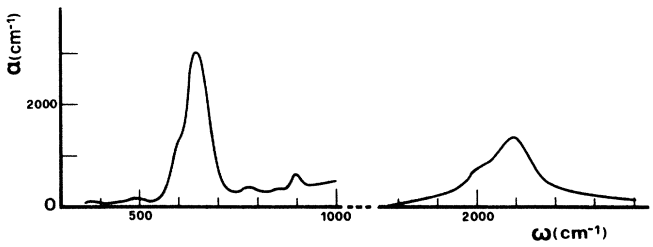

FIG. 3. ir absorption spectrum for the sample Si-*E*52.

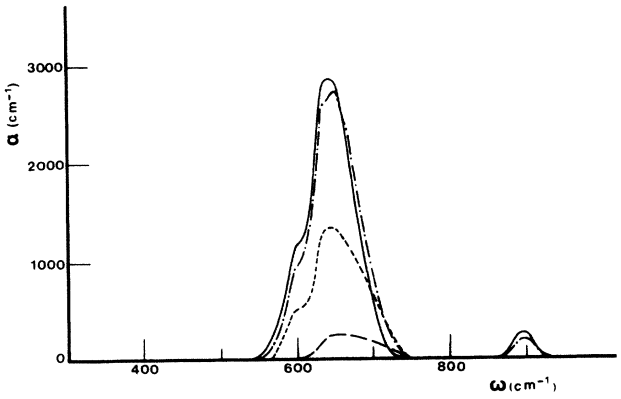

FIG. 4. Absorption coefficient versus frequency for wagging and bending modes in the samples: Si-$E45$ (long-dashed line), Si-$E46$ (short-dashed line), Si-$E47$ (dashed-dotted line), and Si-$E48$ (solid line).

cients versus frequency for stretching modes for the same films are shown in Fig. 5.

The integrated intensities $S_{W,S,B}$ contributing to a specific vibration mode are evaluated using the expression

$$S_{W,S,B}=\int_{W,S,B}\frac{\alpha(\omega)}{\omega}d\omega\ ,$$

where $\alpha(\omega)$ is the absorption coefficient for frequency ω and the integration is over the absorption peak corresponding to the wagging, stretching, and bending vibration modes, respectively.

The ratios of the total hydrogen content as obtained from NR measurements to the integrated intensities of the bands are reported in Table II. When the hydrogen content is low the intensities S_S and S_B are of the order of the experimental errors and then are not reported. In Table II the ratios of the integrated intensities of the different bands: S_S/S_W, S_B/S_W, S_B/S_S, are also reported.

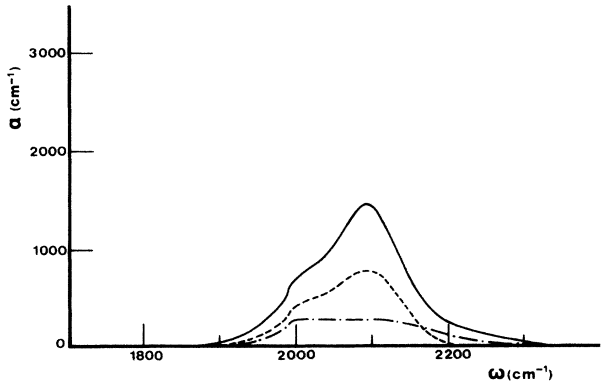

FIG. 5. Absorption coefficient versus frequency for stretching mode in the samples: Si-$E46$ (dashed-dotted line), Si-$E47$ (short-dashed line), and Si-$E48$ (solid line).

It can be seen that as the hydrogen content increases, up to about a saturation, both the bending and stretching modes increase. The number of oscillators for unit volume N can be given by the expression given by Brodsky *et al.*,[2]

$$N=\frac{(1+2\epsilon_m)^2}{q\epsilon_m^2}\epsilon^{1/2}\frac{N_A}{(\Gamma/\zeta)}\int\frac{\alpha(\omega)}{\omega}d\omega \qquad (1)$$

or by the expression given by Connell and Pawlik,[13]

$$N=\frac{q\epsilon^{1/2}}{(\epsilon+2)^2}\frac{N_A}{(\Gamma/\zeta)}\int\frac{\alpha(\omega)}{\omega}d\omega\ . \qquad (2)$$

In Eqs. (1) and (2) we take values of $\epsilon=8$, 10, and 11.6 corresponding to the values of the index of refraction n included in the range of our experimental values; N_A is Avogadro's number and Γ/ζ, the integrated strength of the corresponding band in a gaseous hydride given in cm^2/m mole bond), is taken as 3.5; as in Ref. 2, we calculate the constants A_B of Eq. (1) and A_C of Eq. (2) and f given by

$$A_B=\frac{(1+2\epsilon_m)^2}{q\epsilon_m^2}\epsilon^{1/2}\ ,$$

$$A_{\mathscr{C}}=\frac{q\epsilon^{1/2}}{(\epsilon+2)^2}\ ,$$

$$f_{B,C}=\frac{N_A}{\Gamma/\zeta}A_{B,C}\ .$$

The results are reported in Table III. For samples with hydrogen content of about 1% (i.e., when very little hydrogen is incorporated) it can be supposed that the stretching and bending modes give a very low contribution, as is confirmed by Figs. 4 and 5, and that the probability that the H atom forms a Si—H_1 bond giving a wagging vibration of H atoms roughly normal to the direction of the bond is very high. For that reason it can be supposed that, at very low concentration, the contribution to the spectra from Si-H_1 groups prevails. The values of the constant in Eqs. (1) and (2) for the wagging mode were extracted and compared with the constant obtained experimentally (5.74×10^{19} for Si-$E34$).

The experimental values are in good agreement with the values calculated according to the expression of Connell and Pawlik, while they are different by an order of magnitude from the values obtained according to the expression of Brodsky *et al.* (see Tables II and III).

For higher hydrogen concentrations it can be observed (see Table II) that the integrated intensities of the wagging band increase very slowly while the integrated intensities

TABLE III. Infrared constants.

ϵ	$f(2)$	$f(11)$
8	2.44×10^{20}	4.39×10^{19}
10	2.67×10^{20}	3.41×10^{19}
11.6	2.82×10^{20}	2.86×10^{19}

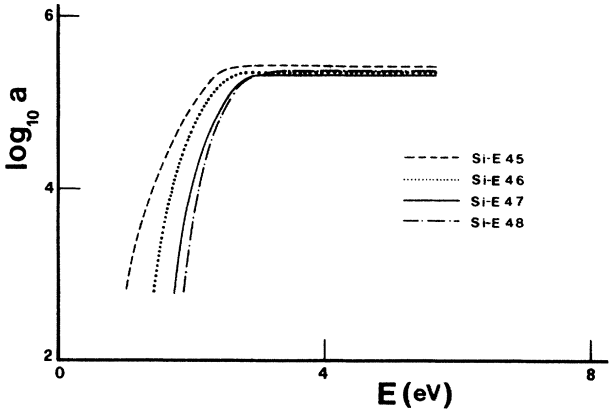

FIG. 6. Spectral dependence of the absorption coefficient α near the band edge for samples with different hydrogen content.

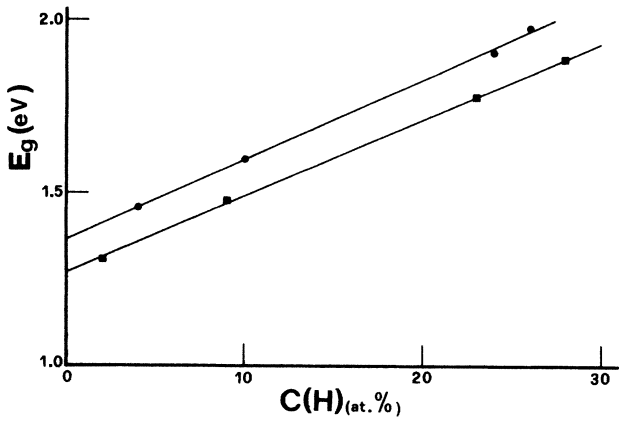

FIG. 8. E_g as a function of hydrogen content for two different substrate temperatures and two different argon pressure: ●, 250°C and $\sim 7.5\times10^{-3}$ mbar; ■, 280°C and $\sim 4.0\times10^{-3}$ mbar.

of the stretching band increase markedly, as is confirmed by the behavior of the S_S/S_W ratios. On the other hand, S_B/S_S is practically constant for the first set of samples. Therefore the higher hydrogen concentration measured by NR can be attributed to the increase of stretching contribution due to the capture of an H atom by Si as SiH_2.

On the basis of these considerations an experimental value of the constant f_s of 2.16×10^{20} was extracted near the values obtained by using Eqs. (1) and (2) as can be seen in Table III. As a conclusion, it does not seem too correct to use a unique value of the constants for all concentrations to calculate the value of hydrogen concentration in α-Si:H films[14] from ir spectra.

C. Optical properties

Techniques developed elsewhere[15] were used to analyze the experimental data of transmittance and reflectance measurements in the uv—visible—near-ir region. Spectral dependence of the absorption coefficient α near the band edge as a function of hydrogen concentration is shown in Fig. 6.

Figure 7 shows the spectral dependence of $(\alpha E)^{1/2}$, where E is the energy, for different hydrogen content. The optical band gaps E_g obtained with the least-squares fit increase linearly as a function of hydrogen content presenting slightly different slopes at different substrate temperatures, as it can be observed from Fig. 8.

The index of refraction n as a function of wavelength for two samples with different hydrogen content is shown in Fig. 9. The index of refraction decreases with increasing hydrogen concentration, indicating a decrease in the polarizability and therefore in the bonding energy of the Si-H network.

Bahl and Bhagat[11] derived the followed expression for the variation in n caused by the variation of the optical band gap E_g:

$$\Delta n = -\frac{c\gamma^2 h}{2\pi^2}\left[1-\frac{E_g}{E_h}\right]^2\frac{\Delta E_g}{E_g}\ , \tag{3}$$

where c is the speed of light, h is Planck's constant, and γ is the slope of the straight lines representing $(\alpha E)^{1/2}$

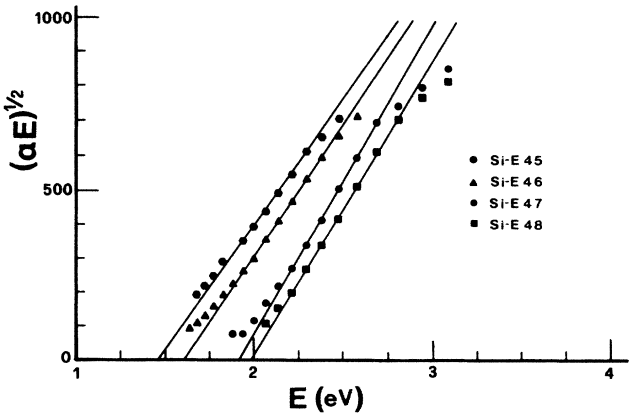

FIG. 7. $(\alpha E)^{1/2}$ versus E for samples with different hydrogen content.

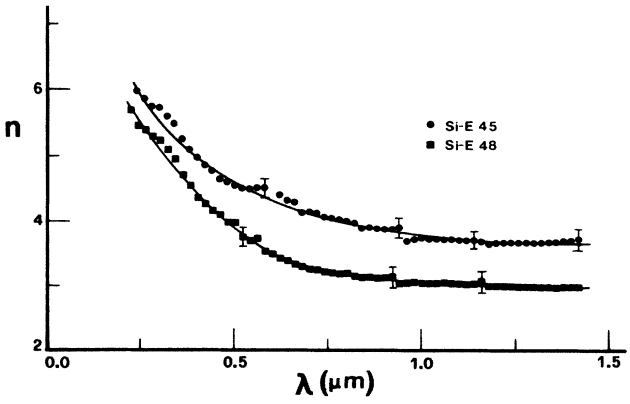

FIG. 9. Index n as a function of λ for samples with different hydrogen content.

versus energy E and whose intercepts with energy axis give E_g. Using a value of 10 eV for $(E_h - E_g)$ the width of the valence band in Si and $\gamma = 500\ \text{cm}^{-1/2}\text{eV}^{-1/2}$ the expression (3) becomes to a good approximation[11]

$$\Delta(\Delta n) \simeq 1.28 \Delta E_g / E_g \ . \tag{4}$$

From measurements of n, E_g, and γ (see Fig. 7) at different hydrogen concentration one can obtain the value of the energy E_h characteristic of the valence band. Yous *et al.*[16] give for E_h a value of 6.4 ± 0.5 eV for films obtained by chemical vapor deposition. We have calculated the value of E_h by using our experimental values of E_g, γ, and n at $\lambda = 1.5\ \mu$m.

We obtain a value of $E_h = 4.76 \pm 0.1$ eV for the set deposited at a temperature of 250 °C and $P_T \cong 9 \times 10^{-3}$ mbar, and $E_h = 4.18 \pm 0.1$ eV for the set at 280 °C and $P_T \cong 5 \times 10^{-3}$ mbar. The differences so obtained confirm the influence of the preparation methods on the physical properties of α-Si:H films.

Further information can be obtained by examining the behavior of experimental values of $n(\lambda)$. The well-known Wemple-DiDomenico model[10] explains the $n(\lambda)$ behavior in the form

$$n^2 - 1 = \frac{E_d E_0}{E^2 - E_0^2} \ , \tag{5}$$

where E_d is the dispersion energy and is proportional to the volume density of valence electrons involved in the transition at E_0, and E_0 is an average interband transition energy.

The plot of $1/(n^2-1)$ versus E^2 has an intercept at $E^2 = 0$ of E_0/E_d and a slope of $-(E_0 E_d)^{-1}$. The results are presented in Table IV. It can be observed that E_d for sample Si-*E*30 ($C_H \sim 1\%$) is comparable to the crystalline silicon value. Our values of E_0 and E_d for the films obtained with a substrate temperature of 250 °C are in agreement with those of de Neufville *et al.*[6] for reactively sputtered films, while those obtained at 280 °C present values of E_0 which are smaller. A systematic decrease in E_d and an increase in E_0 with increasing hydrogen content is similar to those of Zanzucchi *et al.*[17] A monotonic increase of E_0 with hydrogen is expected because of the higher oscillator strength or the bonding energy of the Si—H bond over the Si—Si bond. Furthermore, our results of E_d are in agreement with Wemple's contention of the dependence of E_d on the short-range order.

TABLE IV. Hydrogen content dependence of dispersion energy E_d and average interband transition energy E_0.

Sample	E_d (eV)	E_0 (eV)	T_S (°C)
Si-*E*30	47.82	2.63	280
Si-*E*31	32.87	2.63	280
Si-*E*32	29.54	2.69	280
Si-*E*33	30.51	2.80	280
Si-*E*45	32.50	3.12	250
Si-*E*46	27.77	3.11	250
Si-*E*47	26.49	3.53	250
Si-*E*48	25.98	3.53	250
c-Si	48.38	2.52	

D. Electrical properties

The results of the electrical resistance measurements are reported in Table V. The values so obtained show the influence of hydrogen concentration on the resistivity ρ ($T = 300$ K); activation energies E_a were calculated by the inversion of Arrhenius equation[18]

$$E_a = E_c - E_F - kT \ln(\sigma_0/\sigma_d) \ ,$$

where, following Mott, we take the minimum metallic conductivity σ_0 to be 200 $\Omega^{-1}\,\text{cm}^{-1}$.

The resistivities and the activation energies for the various films are reported in Table V. It can be observed that for hydrogen concentration greater than 25 at. %, ρ decreases slightly. Furthermore, resistivities higher by an order of magnitude are measured for films deposited for ir measurements. A possible explanation is that these films are thicker with respect to those for optical visible measurements.

IV. CONCLUSIONS

An investigation into the physical properties of rf magnetron sputtered hydrogenated amorphous silicon with different substrate temperatures is reported in this study. The absolute content of hydrogen was obtained by nuclear reaction measurements. Identification of the wagging, stretching, and bending mode frequencies in the ir spectra is given. The hydrogen concentrations obtained by NR are compared with the strength of the ir wagging, stretching, and bending bands for a large number of α-Si:H samples; the constants which relate the integrated absorption to hydrogen concentration are obtained. By comparing the calculated and the experimental values of these constants, we deduce that for the wagging band there is a good agreement when the model of Connell and Pawlik is applied while there is a difference by an order of magnitude when we use the model of Brodsky *et al.* Under the same absorption intensity the constant of Brodsky *et al.* gives a greater hydrogen content since a smaller increase of the local field is considered. The constant for the stretching band was obtained for high hydrogen concentration and its value is in agreement with the values calculated according to Brodsky *et al.* and Connell and Pawlik. To calculate the value of hydrogen concentration in α-Si:H films from the measured strength of the ir bands it is convenient to use two different constants: for low hydrogen content, a constant for the wagging band obtained according to the expression of Connell and Pawlik; while for high hydrogen content, the constant for the stretching band obtained according to the expression of Brodsky *et al.* Optical and electrical properties of the films are reported. As the hydrogen concentration increases, the magnitude of the absorption coefficient at a given wavelength decreases, the energy gap increases, and the refractive index decrease over all the wavelengths.

Refractive index dispersion data were analyzed and give

TABLE V. Electrical properties.

Sample	Thickness (Å)	R (Ω)	ρ (Ω cm)	E_a (eV)
Si-E30	2800	2.5×10^{7}	1.82×10^{3}	0.331
Si-E31	3800	1.17×10^{10}	1.16×10^{6}	0.498
Si-E32	3700	1.61×10^{10}	1.55×10^{6}	0.506
Si-E33	4000	9.7×10^{9}	1.01×10^{9}	0.495
Si-E34	23000	4.85×10^{6}	2.9×10^{3}	0.343
Si-E35	23000	5.94×10^{11}	3.55×10^{8}	0.646
Si-E36	20000	1.98×10^{12}	1.03×10^{9}	0.674
Si-E37	20000	5.55×10^{11}	2.89×10^{8}	0.641
Si-E45	3200	1.226×10^{8}	1.02×10^{4}	0.376
Si-E46	3600	4.95×10^{11}	4.63×10^{7}	0.593
Si-E47	4000	9.20×10^{11}	9.57×10^{7}	0.612
Si-E48	3850	7.00×10^{11}	7.01×10^{7}	0.604
Si-E49	32000	3.04×10^{6}	2.53×10^{3}	0.340
Si-E50	27200	3.98×10^{11}	2.81×10^{8}	0.640
Si-E51	26000	2.85×10^{11}	1.93×10^{8}	0.630
Si-E52	13000	2.13×10^{11}	7.20×10^{8}	0.664

information on the simple oscillator energy, the dispersion energy, and characteristic valence-band energy. All these fundamental optical and electrical properties and their hydrogen content are so strongly correlated that, if one is known, the others can be predicted. However, a deeper investigation of the relationship among macroscopic properties (i.e., E_g, n, ...), ir constants, and unit cell structure,[19] at which most of the macroscopic properties are related, seems to be relevant in order to allow the achievement of fixed device performance (i.e., solar-cell efficiency, diode characteristic, etc.), through the control of the structural properties (i.e., type of H bonding, number of dangling bonds, density of localized and unlocalized states, etc.).

ACKNOWLEDGMENTS

The authors acknowledge the technical assistance of Mr. F. Bona, G. Gelo, and L. Macera. The authors are grateful to SIO Divisione Scientifica Blugas, Airliquide, Milano, for kindly providing the gases and the gas handling equipment used in the depositions. This work was partial supported by the Research Project PF2, sponsored by the Consiglio Nazionale delle Ricerche (CNR), Italy, "Unitá di Ricerca No. 24 del Gruppo Nazionale di Struttura della Materia del Consiglio Nazionale delle Ricerche." "Unitá di Ricerca No. 13. del Gruppo Nazionale di Struttura della Materia del Consiglio Nazionale delle Ricerche."

[1]E. C. Freeman and W. Paul, Phys. Rev. B **18**, 4288 (1978).
[2]M. H. Brodsky, M. Cardona, and J. J. Cuomo, Phys. Rev. B **16**, 3556 (1977).
[3]T. D. Moustakas, J. Electron. Mater. **8**, 391 (1979).
[4]D. E. Carlson, *Progress in Crystal Growth Characteristics,* (Pergamon, London, 1981), Vol. 4, pp. 173–193.
[5]P. M. Martin and W. T. Pawlewicz, Sol. Energy Mater. **8**, 391 (1979).
[6]J. P. de Neufville, T. D. Moustakas, A. F. Ruppert, and W. A. Landford, Non-Cryst. Solids **35-36**, 481 (1980).
[7]F. Demichelis, A. Tagliaferro, E. Tresso, and P. Rava, J. Appl. Phys. **57**, 5424 (1985).
[8]F. Demichelis, E. Minetti-Mezzetti, P. Rava, A. Tagliaferro, and E. Tresso, *Proceedings of the Sixth European Photovoltaic Solar Energy Conference, London, 1985* (Reidel, Dordrecht, 1985), p. 702.
[9]F. Demichelis, E. Minetti-Mezzetti, A. Tagliaferro, E. Tresso, P. Rava, and N. M. Ravindra, J. Appl. Phys. **59**, 611 (1986).
[10]S. H. Wemple and M. DiDomenico, Phys. Rev. B **3**, 1338 (1971).
[11]S. K. Bahl and S. M. Bhagat, J. Non-Cryst. Solids **17**, 409 (1975).
[12]M. H. Brodsky, M. A. Frisch, J. F. Ziegler, and W. A. Lanford, Appl. Phys. Lett. **30**, 11 (1977); **30**, 561 (1977).
[13]G. A. N. Connell and J. R. Pawlik, Phys. Rev. B **13**, 787 (1976).
[14]C. J. Fang, K. J. Gruntz, L. Ley, M. Cardona, F. J. Demond, G. Muller, and S. Kalbitzer. J. Non-Cryst. Solids **35**, 36 (1980); **35**, 255 (1980).
[15]F. Demichelis, E. Minetti-Mezzetti, A. Tagliaferro, and E. Tresso, Nuovo Cimento **4**, 68 (1984).
[16]B. Yous, J. M. Berger, J. P. Ferraton, and A. Dormadien, Thin Solid Films **82**, 279 (1981).
[17]P. J. Zanzucchi, C. R. Wronski, and D. E. Carlson, J. Appl. Phys. **48**, 5227 (1977).
[18]P. E. Vanier, A. E. Delahoy, and R. W. Griffith, J. Appl. Phys. **52**, 5235 (1981).
[19]K. Winer and F. Wooten, Phys. Status Solidi B **124**, 473 (1984).